Research Article Vol. 33, No. 5 / 10 Mar 2025 / Optics Express 9804
Optics EXPRESS

Generation of large energy 355 nm ultraviolet light based on a pulse-pumped Nd:YVO4 amplifier with aperture-like structure

YANLIN ZHANG,[1] JIE YANG,[1] XUECHEN CAO,[1] PIXIAN JIN,[1,2] AND HUADONG LU[1,2,*]

[1]State Key Laboratory of Quantum Optics Technologies and Devices, Institute of Opto-Electronics, Shanxi University, Taiyuan 030006, China
[2]Collaborative Innovation Center of Extreme Optics, Shanxi University, Taiyuan 030006, China
*luhuadong@sxu.edu.cn

Abstract: A large energy pulsed 355 nm ultraviolet (UV) light with a pulse repetition rate (PRR) of 10 kHz is presented in this paper, which is implemented by employing a two-stage Nd: YVO_4 master oscillation power amplifier (MOPA) with the aperture-like structure. By optimizing the mode-matching between the seed and pump laser of the amplifiers, an aperture-like structure can be skillfully constructed for the laser crystal. In this case, the amplified spontaneous emission (ASE) can be effectively filtered out, and its influence on the amplified fundamental-wave laser pulse can be eliminated. On this basis, a 355 nm UV light with an average power and energy of up to 40 W and 4 mJ is obtained through third harmonic generation. The achieved pulse width is 7.8 ns. To the best of our knowledge, it is the maximum output power of 10 kHz 355 nm UV light with high beam quality and narrow pulse width realized via Nd: YVO_4 crystals. We think that the presented method is conducive to attaining a large energy UV light with high spectral purity.

© 2025 Optica Publishing Group under the terms of the Optica Open Access Publishing Agreement

1. Introduction

Ultraviolet (UV) radiation play a vital role in precision machining, laser medicine, scientific research and wafer processing due to its advantages of high photon energy and small diffraction limit [1–7]. Especially, high power 355 nm UV light with pulse repetition rate (PRR) of 10 kHz has become an important light source in lots of fields including LiDAR and micro-nano process because it is easier to obtain more information per unit time and work more efficiently with the concern of limited response rate of data acquisition and processing systems. To date, the most effective method to obtain 355 nm light is the third harmonic generation (THG) via 1064 nm laser. And the Nd: YAG crystal is the most popular candidate to attain the 1064 nm laser with PRR at the kilohertz level because of its long fluorescence lifetime of 230 μs. In 2009, David R. Dudley et al. realized a 355 nm UV light with output power up to 160 W at a PRR of 8 kHz via side-pumped Nd: YAG crystal. However, the conversion efficiency from pump to UV was only 5.9%, and the pulse width was about 45 ns. In addition, although thermal birefringence compensation was implemented by inserting a 90 ° rotator between the two side-pumped Nd: YAG crystals, the laser still has a bad beam quality of 16 × 18 in x and y respectively [8]; In 2010, Baitao Zhang et al. also realized a 355 nm UV light with output power of 7.8 W using single side-pumped Nd: YAG crystal at a PRR of 8 kHz. The conversion efficiency from pump to UV was only 4.3%, and the pulse width is 50 ns [9]. In 2014, Hay N et al demonstrated an intracavity frequency-tripled Q-switched Nd: YAG laser incorporating polarization multiplexing to achieve 355 nm light with average power of 220 W and peak power > 0.3 MW at 10 kHz. The pulse width was 65 ns and the beam quality M^2 was 32. The conversion efficiency from pump to UV was 8% [10]. Therefore, the 355 nm lights realized via Nd: YAG crystals have drawbacks of low conversion efficiency, bad beam quality at high power, long pulse width much larger than 10 ns,

#553350 https://doi.org/10.1364/OE.553350
Journal © 2025 Received 17 Dec 2024; revised 13 Feb 2025; accepted 13 Feb 2025; published 25 Feb 2025

Optics EXPRESS

and requirement of compensation for thermal-induced birefringence. On the contrary, the 355 nm UV lights realized via Nd: YVO_4 crystals is just managed to overcome these shortcomings. In 2006, Charles X et al. realized a 355 nm UV light with an output power of 64 W, a pulse width of 31 ns at a PRR of 100 kHz via end-pumped Nd: YVO_4 crystals, corresponding to a pulse energy of 0.64 mJ and a peak power of 0.02 MW. The conversion efficiency from pump to UV was greater than 20% [11]; In 2010, X. Yan et al. realized a 355 nm UV light with an output power of 35.1 W, a pulse width of 15.7 ns at a PRR of 70 kHz via end-pumped Nd: YVO_4 crystals, corresponding to a pulse energy of 0.5 mJ and a peak power of 0.032 MW. The conversion efficiency from pump to UV was 16% and the beam quality in both the x and y directions was 1.1 [12]. However, when the PRR of the fundamental-wave 1064 nm laser is reduced to as low as 10 kHz, most of the inverted Nd^{3+} ions will spontaneously emit to the low energy state due to its short fluorescence lifetime of 90 μs, which further causes a serious depopulation loss. Although employing a pulsed pump source to replace the traditional continuous-wave pump source can overcome this problem, the peak power of pump laser has to be significantly improved to supply a large pulse pump energy. In this case, the optical background noise arising from the amplified spontaneous emission and the surface reflection of optical elements can become more and more severe accompany with the power-scaling up, which will decrease the beam quality and broaden the pulse width of the achieved amplified laser because it is easy to interfere with the seed laser. Moreover, differing from the unidirectional seed laser, the noise propagates in both directions. The reverse propagated noise will seriously influence the output power and stability of the oscillator even though an isolator is placed between the oscillator and amplifiers. Therefore, in this paper, we propose a multistage amplifier with aperture-like structure to realize a high power 355 nm UV light at a PRR of 10 kHz via pulse-pumped Nd: YVO_4 crystals. An electro-optic Q-switched 1064 nm seed laser oscillator is built up to realize an output power up to 22 W, which is scaled up to 120 W by amplifier later, the optical conversion from pump 808 nm to 1064 nm is up-to 42%. In this process, an aperture-like diaphragm is cleverly constructed with the assistance of the different thermal focal length of the Nd: YVO_4 crystals inside and outside the pump region. As a result, the optical noise due to the ASE and reflection of optical elements in two-stage amplifier are effectively suppressed and eliminated by adjusting the radius and divergence angle of the seed laser. Based on the prepared 1064 nm laser, an efficient 355 nm UV light with high beam quality and large energy is realized through the THG process, the maximal energy of the single pulse is up-to 4 mJ which is the highest value for a nanosecond laser with a PRR of several kilohertz based on the Nd:YVO_4 crystal, to the best of our knowledge.

2. Theoretical analysis

When the multi-stage pulse-pumped Nd: YVO_4 amplifier is built for scaling up the power of the fundamental-wave laser, the population inversion inside the gain medium is formed rapidly within the pump holding time because of the high peak power of the pump laser. In order to convert the pump to seed laser as much as possible, the seed laser pulse usually arrives while the interaction between pump laser and the gain medium is just completed. However, the inverted particles will spontaneously emit to the low energy state during pumping, which can directly result in a severe ASE. Although the most part of the ASE can be significantly suppressed when the seed laser arrives, the residual ASE still exists and can be cascaded amplified because the generation of the ASE always precedes the arriving of the seed laser. As a result, with the increase of the amplification stage, the amplification ability of the ASE will be larger than that of the seed laser. Since the ASE is strongest at the end of the pumping laser, the front half of the seed laser pulse will be severely broadened by the cascade amplified ASE. At the same time, the amplified ASE can be superimposed on the seed laser in space, which will reduce the beam quality of the amplified laser.

Optics EXPRESS

When a seed laser mixed with the ASE is injected into the amplifier together with a pump laser with top-hat distribution, the thermal lens of the gain medium can be written as [13]

$$f_{th}(r) = \begin{cases} \frac{2\pi K_c \omega_p^2}{P_p \gamma \eta_{abs}(dn/dT)} & (r \le \omega_p) \\ \frac{2\pi K_c r^2}{P_p \gamma \eta_{abs}(dn/dT)} & (r > \omega_p) \end{cases} \tag{1}$$

Where r is the radial coordinate of transverse position, ω_p is the pump beam radius, K_c is the thermal conductivity of the laser material, P_p is the incident pump power, η_{abs} is the fraction of pump power absorbed in the laser rod, $\frac{dn}{dt}$ is the change of refractive index with temperature and γ is the fraction of absorbed pump power dissipated as heat.

When a beam with beam radius and divergence angle (r_0, θ_0) passes through the thermal lens and continuously propagates with a distance of l_2, the new beam radius and divergence angle (r', θ') can be calculated according to the theory of matrix optics, which is written as

$$\begin{cases} r' = l_2\theta_0 - r_0(l_2/(\zeta\omega_p^2) - 1) \\ \theta' = \theta_0 - r_0/(\zeta\omega_p^2) \end{cases} \quad (r \le \omega_p). \tag{2}$$

$$\begin{cases} r' = l_2\theta_0 - r_0(l_2/(\zeta r_0^2) - 1) \\ \theta' = \theta_0 - 1/(\zeta r_0) \end{cases} \quad (r > \omega_p). \tag{3}$$

Where ζ is defined as

$$\zeta = \frac{2\pi K_c}{P_p \gamma \eta_{abs}(dn/dT)} \tag{4}$$

Figure 1 shows the evolution of new beam divergence angle θ' versus r_0 under the same θ_0. There is only one minimum of θ' where $r_0 = \omega_p$. Therefore, once the minimum θ' is zero, the beam with radius ω_p will propagate with a nearly constant radius, but the radii of other beams will diverge larger and larger as the propagation distance l_2 increases.

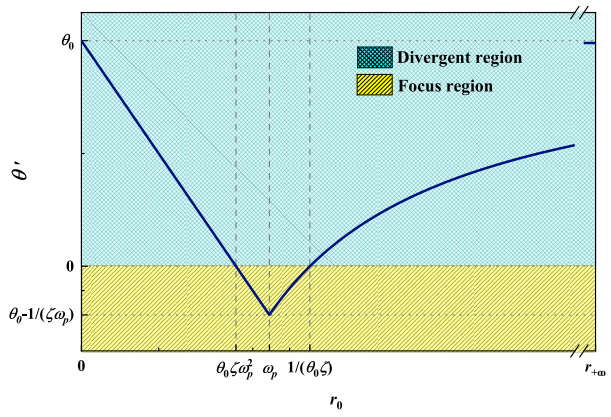

Fig. 1. The new divergence angle θ' after passing through a thermal lens.

It can be assumed that the beam radii and divergence angles of seed light and ASE are (ω_s, θ_s) and (ω_n, θ_n), respectively. Owing to the different generation mechanisms, ω_s and θ_s are often smaller than ω_n and θ_n. Additionally, in order to convert the pump energy to that of the seed laser, it is expected that the beam radii of the pump laser and seed laser beams are the same, i. e. $\omega_p = \omega_s$. In this case, when $\theta_s' = 0$, after passing through the gain medium and propagating with

Optics EXPRESS

the distance l_2, the beam radius variation of the seed and ASE with the propagating distance l_2 can be attained and illustrated in Fig. 2, where a_1-a_4 and b_1- b_5 represent the ray within the seed laser and ASE beam radii, respectively. It is clear that the seed laser inside the pump region can well propagate along the pumping region while the ASE mixed with the seed light rapidly spread beyond the pumping area due to the large thermal lens effect inside the pumping region and its large divergence angle. For the ASE outside of the pumping region, it directly diverges since the thermal lens effect outside the pumping region is relatively small. From Fig.2, it can be found that an aperture-like structure can be directly constructed in the gain medium of the amplifier to effectively filter out the ASE and achieve efficient and stable seed laser amplification with the assistance of the different thermal effects of the gain medium inside and outside the pump region as well as the large divergence angle of the ASE.

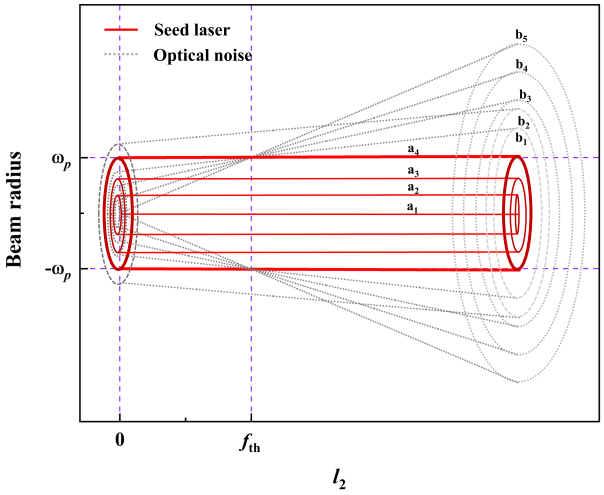

Fig. 2. The filtering effect of the aperture-like structure (the new beam radius r' varies with l_2).

3. Experimental setup

The experimental setup to implement the high power 355 nm UV light with the PRR of 10 kHz is illustrated in Fig. 3. The seed laser is acted by a homemade electro-optic Q-switched pulsed 1064 nm laser with the PRR of 10 kHz. The maximal output power and pulse width are 22 W and 9.78 ns, respectively. The output seed laser beam is firstly reshaped by a coupling system consisting of f_1 (315 mm), f_2 (−200 mm) and f_3 (−150 mm). An optical isolator (ISO, CASTECH INC) is placed between the f_1 and f_2 to avoid the feedback of the amplifier. In order to scale up the power of the fundamental-wave 1064 nm laser, a two-stage pulse-pumped amplifier is designed and built, where two cascade Nd: YVO_4 laser crystals are employed for every stage of the amplifier. The cross sections and lengths of the Nd: YVO_4 laser crystals are 4×4 mm^2 and 20 mm which include undoped length of 3 mm and doping length of 17 mm. To effectively scale up the power of the seed laser and control the thermal lens effect for constructing an aperture-like structure, the doping concentrations of the laser crystals are 0.2at. %. Both surfaces of the laser crystals are coated with anti-reflection (AR) film at 1064 nm and 808 nm. At the same time, in order to eliminate the generation of parasitic oscillation, a wedge angle of 2° is designed and cut on the rear surfaces of the laser crystals. Four fiber-coupled semiconductor lasers with a central wavelength and output power of 808 nm and 200 W, respectively are employed to act as the pump sources. Their core diameters and numerical apertures are 400 μm and 0.22, respectively. The

Optics EXPRESS

current of power supply for achieving the output power of 200 W is 12 A. In order to satisfy the requirements of the pulse pumping, the current provided by power supply is modulated by a rectangular signal with a repetition rate and duration of 10 kHz and 30 μs, respectively. In this case, the current waveform is rectangular, with a full width at half maximum (FWHM) of 28.81 μs. The rise and fall times (10-90%) of the current are 4.12 μs and 5.39 μs, respectively. The output waveform of the pump laser is also rectangular, with a little narrower FWHM of 24.12 μs. The rise and fall times (10-90%) of pump waveform are 3.42 μs and 2.45 μs, respectively. The average pump power output from the coupled optical fiber is measured to be 58 W, thus the peak power obtained by dividing the measured average power by the FWHM and repetition rate is about 240 W. In the experiment, considering the optical conversion efficiency and the damaged threshold of the laser crystals as well as the suppression of the parasitic oscillation, the beam radius of the seed laser injected into the amplifier is optimized to 0.8 mm at the incident end face of Nd: YVO_4. At the same time, the beam radius of every pump beam is also optimized to 0.8 mm at the incident end face of Nd: YVO_4 by a coupling system including two lenses with focal length of 20 mm and 80 mm, respectively (f_7 - f_{14}). The laser beam output from the first stage of the amplifier is coupled into the second stage of the amplifier by a coupling system consisting of f_4 (500 mm), f_5(−150 mm) and f_6 (−150 mm). The amplified laser beam from the amplifier is injected into the frequency-doubling and sum-frequency module to generate the 355 nm UV light. The frequency-doubling crystal LBO_I is cut at $\theta = 90°$, $\varphi = 0°$ for type-I noncritical phase-matching with the size of $3 \times 3 \times 20$ mm^3 and it is placed in a copper oven where the temperature is precisely controlled to 148 °C. Both surfaces are coated with the AR films at 1064 nm and 532 nm. The sum-frequency crystal LBO_{II} is cut at $\theta = 42.2°$, $\varphi = 90°$ for type-II critical phase-matching with a size of $3 \times 7 \times 20$ mm^3 and it is also placed in a copper oven where the temperature is precisely controlled to 28 °C. Both surfaces are coated with the AR films at 1064 nm, 532 nm and 355 nm. To compensate for the walk-off effect of the critical phase-matched crystal, both ends of the sum-frequency crystal are cut with an angle of 17 ° [14].

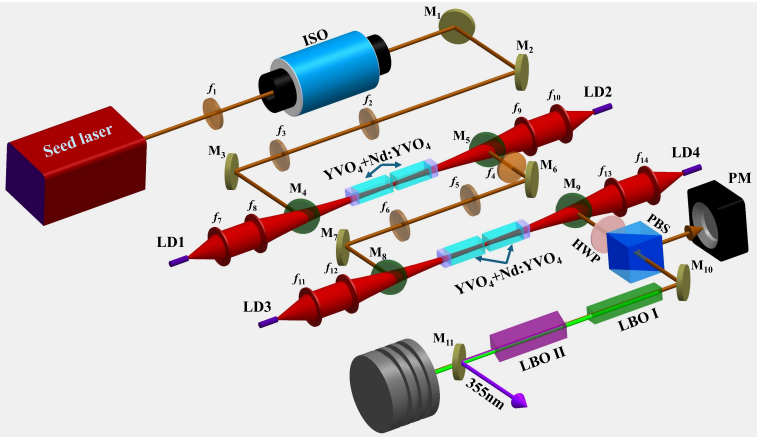

Fig. 3. Schematic diagram of high power 355 nm UV light with PRR at 10 kHz.

4. Results and analysis

After the whole experimental system was aligned, the ASE was unavoidable to generate and amplified along with the amplification of the seed laser because of the arrival time delay between the seed and the pump pulses, which would directly influence the conversion of the 355 nm UV light. Therefore, an optimal coupling system must be placed before the first and second stages of the amplifier for forming an effective aperture-like structure to filter out the noise as much

Optics EXPRESS

as possible. In the experiment, the coupling systems consisting of four lenses (f_1-f_2, f_4-f_5) were firstly placed before the two amplifying stages. In this case, the beam radius of the seed laser and the pump laser are both 0.8 mm at the incident end face of Nd: YVO_4 crystal. Figure 4(a) showed the beam propagation diagram of 1064 nm laser from the seed to M_5. The variations of the pulse width and the intensity distribution were recorded when the oscillator and the two amplifiers were all working. The recorded results were depicted in Fig. 5(a), where areas I and II were defined as the rising edge and the pulse falling edge of the 1064 nm laser pulse, respectively. It can be seen that the pulse width of the injected seed laser was 9.68 ns, and the cross-section intensity distribution of the seed laser beam was basically a standard Gaussian distribution. However, after one-stage amplification, the pulse width of the laser was expanded to 10.08 ns. Moreover, the pulse rising edge in area I was no longer smooth, which meant that the laser pulse has obviously been mixed by the noise modulation signal. After secondary amplification, the pulse width was further widened to 10.53 ns, and the front half of the pulse was even more uneven. At the same time, the intensity distribution of the laser beam has been severely disturbed by the ASE after two-stage amplification. On the contrary, when two concave lens with focal length of 150 mm (f_3 and f_6) were inserted after the existing coupling systems to compensate the thermal focal length inside the pump region and the beam radius of the seed laser at the incident end face of Nd: YVO_4 remain unchanged by adjusting the focal length and position of the lens in the coupling system, the gain crystal would automatically form an obvious aperture-like structure due to the thermal lens effect. Figure 4(b) showed the beam propagation diagram of 1064 nm laser from the seed to M_5 after the 150 mm concave lens installation. From Fig. 5(b), it can be seen that the pulse width and the intensity distribution were basically same as that of the injected seed laser. What's more, the modulated signals have been eliminated and the pulse rising edge was still very smooth. The experimental results showed that constructing an aperture-like structure based on the thermal lens effect of the laser crystals in the amplifier pave a way to filter out the ASE and improve the spectral purity of the laser.

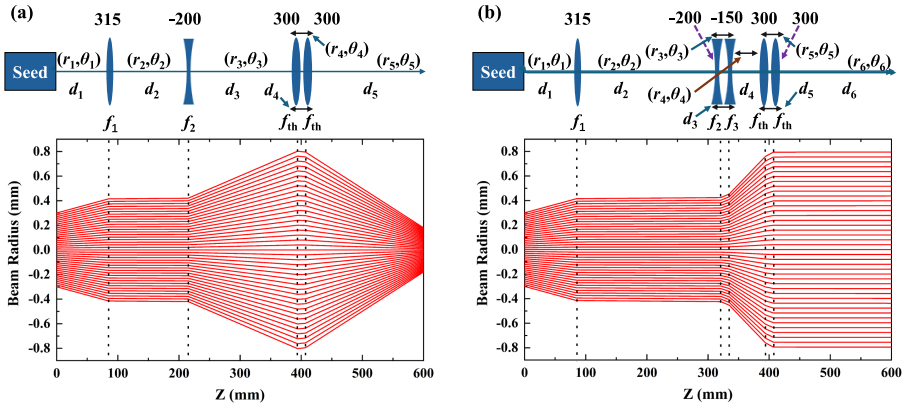

Fig. 4. The beam propagation diagram of 1064 nm laser from the seed to M_5 before (a) and after (b) the 150 mm concave lens installation with the horizontal axis position and vertical axis beam radius.

On this basis, a stable pulsed 1064 nm laser with high performance was achieved, whose output characteristics were recorded and shown in Fig. 6. Firstly, the power of the seed laser was scaled up to 120 W based on the optimized two-stage amplifier, as shown in Fig. 6(a). In the first amplifier, the amplified laser was not constrained by the crystal apertures because the distance between the adopted concave lens f_3 and the crystal was only about 60 mm. However, when the amplified laser was injected into the second amplifier, it was easy to be blocked by the crystal apertures of the second amplifier when the pump power was low. Therefore, we measured

Optics EXPRESS

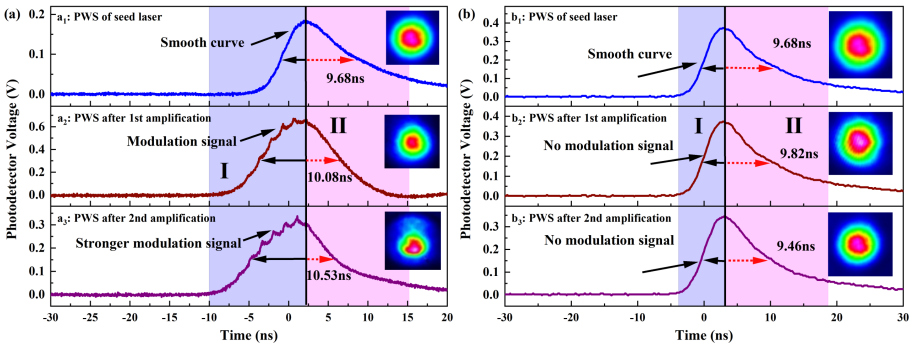

Fig. 5. The evolution of 1064 nm pulse waveform and background optical noise around the seed laser without aperture-like construction (a), and with aperture-like construction (b).

the power just after the first amplifier. However, the power after the second amplifier must be measured only if the first amplifier worked with the maximal power. The pulse width and the PRR of the achieved 1064 nm laser was 9.46 ns, which was the same as that of the seed laser, as shown in Fig. 6(b). The root-mean-square (RMS) value of the output power of 1064 nm laser within 4.5 hours is 0.13%, as shown in Fig. 6(c), the inset showed a stable pulse train of 1064nm laser. The beam quality M^2 in x and y directions were 1.22 and 1.17, which was obtained by recording the caustic curves depicted in Fig. 6(d), where the beam diameter in Fig. 6(d) was measured with $1/e^2$ criterion. It can be seen that the beam quality is not degraded, although the output power has been amplified to 120 W, which can mainly ascribe to the efficient filtering effect of the aperture-like structure.

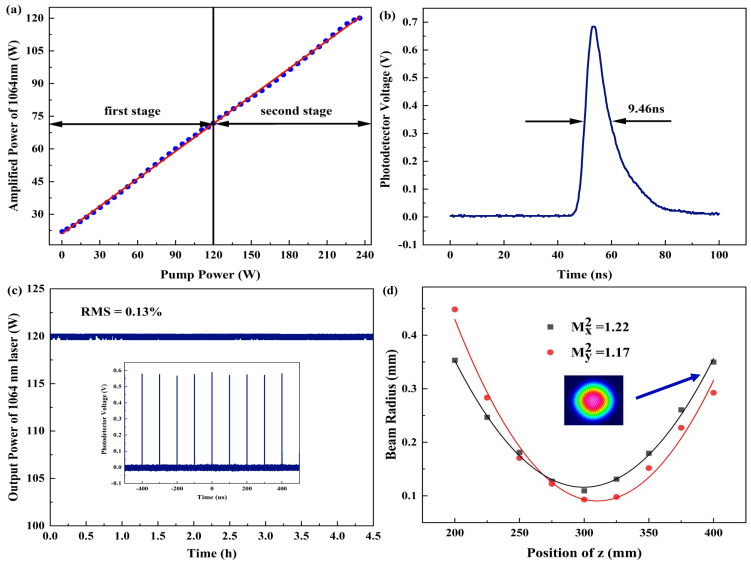

Fig. 6. The amplified power of 1064 nm laser versus pump power (a), pulse waveform with no modulated signal (b), power stability of 1064 nm laser (the inset shows the pulse train of 1064 nm laser) (c) and beam quality M^2 (d).

The amplified 1064 nm laser successively passed through the cascaded type-I phase-matched LBO_I and type-II phase-matched LBO_{II} to generate 355 nm UV light. As a result, the maximum output power of 355 nm light is up-to 40 W, the output power trend curve of 532 nm light and 355

Optics EXPRESS

nm light were illustrated in Fig. 7(a). The optical conversion efficiency from 1064 nm to 355 nm was 33.3%. The pulse width and PRR of the achieved 355 nm UV light were 7.8 ns, as shown in Fig. 7(b). It can be known that the energy and the peak power can reach up-to 4 mJ and 0.5 MW, respectively. To the best of our knowledge, it was the highest value of the achieved 355 nm UV light with the PRR of 10 kHz realized via Nd: YVO_4 crystals. Especially, the beam quality M^2 in the x and y directions were better than 1.5 and 1.6, respectively, as shown in Fig. 7(c). The RMS value of the output power of 355 nm light within 4.5 hours is 0.74%, as shown in Fig. 7(d).

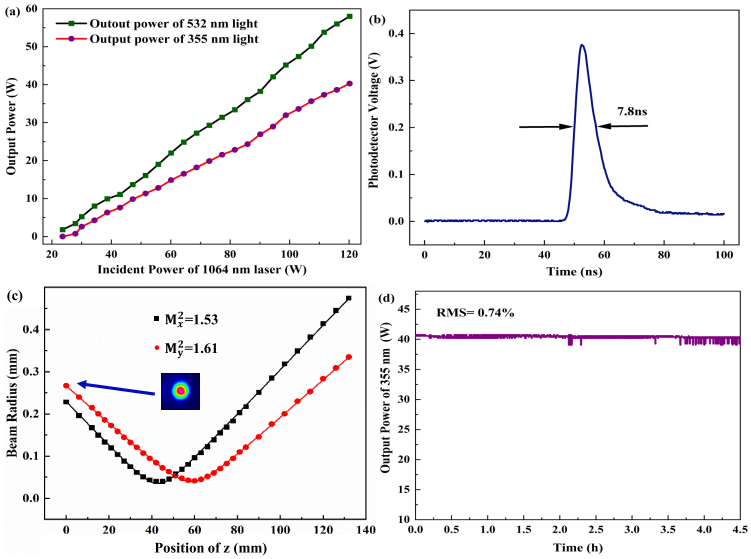

Fig. 7. Output power of 532 nm light and 355 nm light versus incident power of 1064 nm laser (a), pulse waveform of 355 nm (b), beam quality M^2 (c) and power stability of 355 nm light (d).

5. Conclusion

We report a 10 kHz 355 nm UV light via Nd: YVO_4 crystal with high power, high efficiency, high beam quality and narrow pulse width. A two-stages dual end-pumped Nd: YVO_4 amplifier with aperture-like structure was proposed to suppress and eliminate the ASE and reflected feedback by optical elements under high gain, permitting the generation of high-power 1064 nm laser. The 355 nm UV light with high beam quality was generated through THG of the prepared high power 1064 nm laser. In the experiment, a 1064 nm seed laser with an output power up to 22 W, a PRR at 10 kHz, and a pulse width of 9.68 ns were realized by an electro-optic Q-switched oscillator. Then, the seed laser was scaled up to 120 W by a two-stages dual end-pumped amplifier with aperture-like construction. The extraction efficiency from the average pump power to the output power of 1064 nm laser was as high as 42%. On this basis, a 355 nm UV light with an average power up to 40 W, a pulse width of 7.8 ns, and an optical-to-optical efficiency of 33.3% were obtained through THG. Compared with the traditional 10 kHz 355 nm light realized via Nd: YAG crystals, this laser not only has a much better beam quality, a higher optical efficiency by more than twice, a shorter pulse width by five times, but also is more compact and cost-effective, which can further satisfy the demands of high resolution and better processing effect in LiDAR and micro-nano process. More importantly, this method enables the generation of several kilohertz repetition rate lasers with high-efficiency and large energy based on Nd: YVO_4 crystals and

Optics EXPRESS

provides guidance for other crystals with short fluorescence lifetimes to obtain large energy output.

Funding. National Key Research and Development Program of China (2022YFC2204003); Applied Basic Research Project of Shanxi Province, China (No. 202103021221004); Shanxi Scholarship Council of China (No. 2022-015); Science and Technology Innovation Group of Shanxi Province (202204051002005); The first Lab - National Innovation Center (Shanxi) science and technology innovation project; Funding from the National Key Laboratory of Particle Transport and Separation Technology (KWKF-2024-2).

Disclosures. The authors declare no conflicts of interest.

Data availability. Data underlying the results presented in this paper are not publicly available at this time but may be obtained from the authors upon reasonable request.

References

1. W. K. Yung, J. Liu, H. C. Man, *et al.*, "355 nm Nd: YAG laser ablation of polyimide and its thermal effect," J. Mater. Process. Technol. **101**(1-3), 306–311 (2000).
2. D. Karnakis, G. Rutterford, and M. Knowles, "High power DPSS laser micromachining of silicon and stainless steel," in *Proceedings of the third international WLT-conference on lasers in manufacturing*, (2005).
3. W. Y. Cheng, C. Feng, F. P. Zhen, *et al.*, "High-average-power third harmonic generation at 355 nm with CsB_3O_5 crystal," Chin. Phys. Lett. **22**(6), 1426–1428 (2005).
4. F. Zhang, J. Duan, X. Zeng, *et al.*, "355nm DPSS UV laser micro-processing for the semiconductor and electronics industry," in *Laser Applications in Microelectronic and Optoelectronic Manufacturing XV*, vol. 7584 (SPIE, 2010), pp. 164–173.
5. T. Rauch and R. Delmdahl, "Advanced UV lasers enable precision processing: UV lasers exhibit high spatial resolution and minimal thermal damage to surrounding material," Laser Tech. J. **6**(3), 20–24 (2009).
6. J. Bovatsek, A. Tamhankar, and R. Patel, "UV lasers improve PCB manufacturing processes," Laser Focus World **48**, 48–52 (2012).
7. T. Li, C. Guo, and C. Zhang, "Design of high energy single longitudinal mode 355 nm UV laser," in *Journal of Physics: Conference Series*, vol. 2459 (IOP Publishing, 2023), p. 012094.
8. D. R. Dudley, O. Mehl, G. Y. Wang, *et al.*, "Q-switched diode-pumped Nd: YAG rod laser with output power of 420W at 532nm and 160W at 355nm," in *Solid State Lasers XVIII: Technology and Devices*, vol. 7193 (SPIE, 2009), pp. 261–268.
9. B. T. Zhang, H. T. Huang, J. F. Yang, *et al.*, "Generation of 7.8 W at 355 nm from an efficient and compact intracavity frequency-tripled Nd: YAG laser," Opt. Commun. **283**(11), 2369–2372 (2010).
10. N. Hay, N. Slavinskis, A. M. Rodin, *et al.*, "> 220 W output power at 355 nm from a Q-switched diode-pumped solid-state laser," in *Solid State Lasers XXIII: Technology and Devices*, vol. 8959 (SPIE, 2014), pp. 105–110.
11. C. X. Wang, G. Y. Wang, A. V. Hicks, *et al.*, "High-power Q-switched TEM_{00} mode diode-pumped solid state lasers with > 30 W output power at 355 nm," in *Solid State Lasers XV: Technology and Devices*, vol. 6100 (SPIE, 2006), pp. 335–348.
12. X. Yan, Q. Liu, H. Chen, *et al.*, "35.1 W all-solid-state 355 nm ultraviolet laser," Laser Phys. Lett. **7**(8), 563–568 (2010).
13. W. Clarkson, "Thermal effects and their mitigation in end-pumped solid-state lasers," J. Phys. D: Appl. Phys. **34**(16), 2381–2395 (2001).
14. X. Yan, Q. Liu, C. Pei, *et al.*, "High-power 355 nm third-harmonic generation with effective walk-off compensation of LBO," J. Opt. **16**(4), 045201 (2014).